

by M. Kirschning*, R.H. Jansen and N.H.L. Koster

University of Duisburg, Department of Electrical Engineering, FB9/ATE

Bismarckstraße 81, D-4100 Duisburg 1, W. Germany

*On the leave to Honeywell GmbH, Dept. VV, PO 1081, D-6457 Maintal 1, W. Germany

ABSTRACT

The broad-band characterization of microstrip discontinuities by an improved resonator technique is described. This technique involves hitherto unknown expressions accounting for nonsymmetrical gap coupling and employs an efficient error function for the computer-aided modeling of microstrip n-ports. It is applied to derive new analytical results for microstrip corners and chamfered right-angle bends.

INTRODUCTION

Resonator methods and associated modeling techniques represent an important tool for the experimental characterization of microstrip parameters and discontinuities where reliable theoretical data are not available¹⁻³. They take advantage of the fact that frequency is a physical quantity which can be measured very accurately even in the microwave and millimeterwave region. On the other hand, in these methods great care is required in the derivation of discontinuity data from the measured resonance frequencies. This is due to statistical variations which are always present in the necessary test configurations. In addition, model uncertainties become noticeable in the problem of de-embedding a discontinuity from a given resonating microstrip structure. To overcome some of these difficulties, cumbersome procedures like successive chemical etching and remeasuring have been employed in the past^{3,4}. However, computerized methods which are much more convenient in view of measurement hardware preparation seem also feasible, and papers published very recently show that theoretical, practical and conceptual aspects of microstrip resonator techniques are under consideration for further improvement⁵⁻⁷. A common feature of these recent contributions is that they use straight rather than ring resonators, for the latter see e.g. ref. 8. Also, these new techniques do not require the independent determination of the microstrip open-end effect. Especially, the methods described in refs. 5 and 7 are characterized by an extreme ease of application and sample preparation. In addition, the technique outlined in ref. 7 has the advantage of generality and eliminates completely the need for an accurate realization of prescribed geometrical dimensions of the considered samples. It is part of a comprehensive approach to the computer-aided design (CAD) of linear microwave integrated circuits (MICs) developed by one of the authors. This technique has been further improved, and rigorous numerical hybrid mode computations⁹⁻¹¹ which establish another part of the mentioned CAD approach have been employed to supply it with accurate a priori data. Details of the improved resonator method and its application to a particular example are demonstrated in the following.

OUTLINE OF THE METHOD

An important feature of the technique described here is the utilization of accurate analytical models with broad range of validity for all those microstrip parameters which are relevant for the evaluation of discontinuity data from the measured resonance frequencies. The appropriate mathematical expressions have been derived by now. They include formulas for the open end effect¹², the frequency dependent effective dielectric constant of microstrip¹³ and the frequency dependent power-current formulation of microstrip characteristic impedance¹⁴. Meanwhile, for the end-to-

end coupling of straight microstrip resonators via a gap involving unequal widths of the adjacent strips numerical data have also been generated. Explicit mathematical formulas deduced from such data are presented as part of this paper. With these expressions, the effect of coupling on the resonance frequencies of a test configuration can be taken into account which results in increased measurement accuracy. A practical advantage of the gap formulas is, that they allow to improve the signal-to-noise ratio in a measurement setup, which is not possible if one has to arrange with loose coupling conditions.

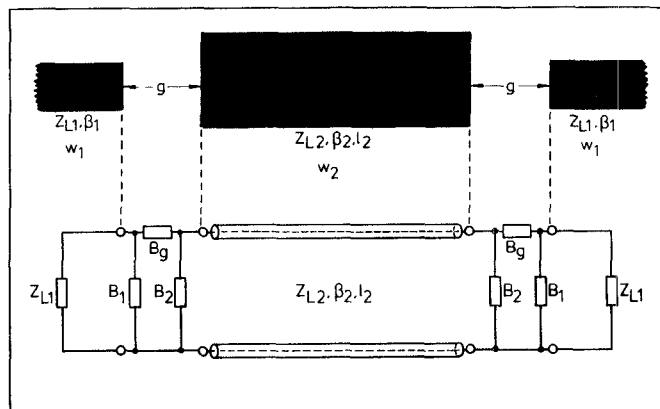


Fig. 1: Basic resonator measurement configuration and associated equivalent circuit

The basic type of test configuration and its equivalent circuit as used in the improved resonator method are shown in fig. 1. The resonance frequencies are measured with a digital frequency meter by detection of the transmission peaks on a network analyzer. The configuration of fig. 1 which contains just a straight resonating length of microstrip is applied here for the accurate determination of the dielectric constant ϵ_r of the substrate pieces considered. By this, it plays a similar role as the reference lines employed by Rizzoli and Lipparini⁵. The difference, however, is that the necessary very accurate specification of the phase constant of the microstrip lines involved in discontinuity measurements is achieved here with the aid of the frequency dependent expressions of ref. 13. The dielectric constant ϵ_r is considered here as a somewhat variable parameter and is adjusted by optimization with respect to the measured resonance frequencies. The advantage is that the widths of the reference lines need not be accurately made the same as of those involved in the discontinuity test structures. Since the functional dependencies of the equivalent

circuit elements of fig. 1 with respect to geometry, dielectric constant and frequency are all known with high accuracy, it is sufficient in the method described here to determine these physical parameters in the actual measurements. It is not necessary to prescribe them in advance to be etched very precisely. With the complete knowledge of the circuit elements of fig. 1, the resonator experiment can be simulated with high precision and computer-aided modeling of low-loss n-port discontinuities can be performed in the way described in ref. 7 and further outlined here by an example.

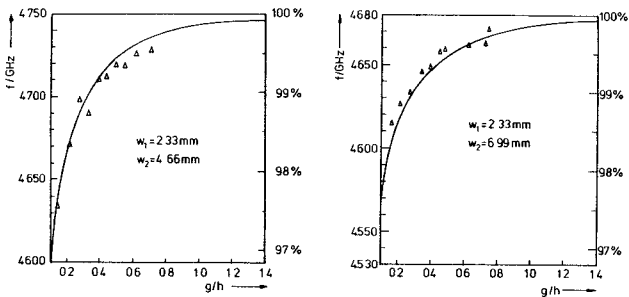


Fig. 2: Comparison between measured ($\Delta\Delta\Delta$) and calculated (—) resonance frequencies for the configuration of fig. 1

The high measurement accuracy achieved becomes obvious from fig. 2 for the case of a plastic substrate (thickness $h = 0.84$ mm, $\epsilon_r = 2.36$, nominal resonator length $l_2 = 20.9$ mm). The maximum relative error magnitude visible there, taken over a total of 20 samples with two nominal resonator widths w_2 and varying coupling gaps g , is approximately 0.25 %. This corresponds well to the local variations of the dielectric constant which have to be expected for the substrate type used. Furthermore, this is an indicator of the quality of the analytical models employed in the numerical simulation of the microstrip test structures. The effect of coupling on the two resonances considered in fig. 2 is of the order of magnitude of 0.1 % if typical loose coupling conditions near $g/h=0.8\dots 1$ prevail. This includes the effect of loading by the external impedances Z_{L1} which have nominal values of 50 Ohms presented by the ports of the employed network analyzer. A numerical study reveals that the influence of slight mismatch, introduced for example by the coaxial-to-microstrip transitions of the measurement setup, can be neglected as long as coupling is not extremely tight. A quantitative description of the non-symmetrical microstrip coupling gap shall be given here only for the range of substrate dielectric constants $6 \leq \epsilon_r \leq 13$ due to restricted printing space. For these values of ϵ_r , the susceptances describing the microstrip gaps in fig. 1 can be written as

$$B_g/mS = Q_1 \cdot \pi(f/\text{GHz}) \cdot (h/\text{mm}) \cdot \exp(-1.86 g/h) \cdot \quad (1)$$

$$(1 + 4.19(1 - \exp(-0.785(h/w_1)^{0.5} \cdot w_2/w_1))),$$

$$B_1/mS = 2\pi \cdot (f/\text{GHz}) \cdot (C_1/\text{pF}) \cdot (Q_2 + Q_3)/(1 + Q_2),$$

$$B_2/mS = 2\pi \cdot (f/\text{GHz}) \cdot (C_2/\text{pF}) \cdot (Q_2 + Q_4)/(1 + Q_2)$$

with the auxiliary quantities

$$Q_1 = 0.04598 \cdot (0.03 + (w_1/h)^{1.23} / (1 + 0.12(w_2/w_1 - 1)^{0.9})) \cdot (0.272 + 0.07 \epsilon_r) \quad (2)$$

$$Q_2 = 0.10700 \cdot (w_1/h + 9) \cdot (g/h)^{3.23} + \\ + 2.09 \cdot (g/h)^{1.05} \cdot (1.5 + 0.3 w_1/h) / (1 + 0.6 w_1/h), \\ Q_3 = \exp(-0.5978(w_2/w_1)^{1.35}) - 0.55, \\ Q_4 = \exp(-0.5978(w_1/w_2)^{1.35}) - 0.55.$$

The abbreviations C_1 and C_2 denote the open-end capacitances of the involved microstrips of widths w_1 and w_2 , respectively. They are computed according to the formulas of refs. 12, 13, 14. The above expressions are valid for the range of geometrical parameters $w_1/h = 0.1 - 3.0$, $w_2/h = 0.1 - 3.0$, $w_2/w_1 = 1 - 3$ and $g/h = 0.2 - \infty$. They are based on numerical data which have been generated by a rigorous spectral domain method^{10,11,15} for a frequency of $f = 4$ GHz and a substrate thickness of $h = 0.635$ mm. With respect to this reference source, they do not deviate by more than an absolute error of 0.1 mS for $w_1/h > 1$ and considerably less for smaller widths w_1 . For other frequencies up to about 18 GHz respectively for $f \cdot h$ products up to approximately 12 GHz \cdot mm, the accuracy of the above gap model is not substantially different. To the experience of the authors, the influence of this model uncertainty can be neglected in the described method.

Beyond the details outlined by now, another important feature of the presented resonator technique consists in the error function used for the computer-aided modeling of discontinuities. This is directly related to the resonator experiment and its numerical simulation in terms of scattering parameters and thus introduces mathematical and conceptual advantages⁷. With the resonance condition

$$\det((S'(f_{ik}))_i - (I)) = \det_{ik} = 0 \quad (3)$$

this error function is formulated according to ref. 7 as

$$F_p = \left(\frac{1}{MN} \sum_{i=1}^M \sum_{k=1}^{N_i} \left| \det_{ik}((X)) \right| ^p \right)^{1/p}. \quad (4)$$

It is of the least-pth type and has to be minimized with respect to the vector of model parameters (X) which symbolically represents the description of an n-port discontinuity. The discontinuity to be modelled, together with properly chosen lengths of open-ended microstrips attached to its ports, is operated as a transmission test resonator between two of the open ends^{6,7}. This is done in the same way as with the basic test configuration of fig. 1. In the error function (4) a total of M test samples, i.e. M different geometries of the considered microstrip structure, contributes to the value of F_p . Each of the samples is characterized by a number of N_i of measured resonance frequencies f_{ik} . The scattering matrix $(S'(f_{ik}))_i$ of the i th test configuration is evaluated with respect to reference planes which coincide with the ends of the two exterior microstrip coupling lines (denoted 1 in fig. 1) and the eventually remaining open ends (hypothetical ideal open end positions), respectively. The exterior load impedances (Z_{L1} in fig. 1) are absorbed into the n-port so that it appears ideally open-circuited at all ports. For this reason, the identity matrix (I) is introduced into the resonance condition (3) to account for the reflections at the ports of a transmission test resonator. For passive n-ports, the contributions \det_{ik} to the error function F_p can be shown to be well behaved and bounded. In the lossless case, the vanishing of F_p is necessary and sufficient to achieve a

perfect fit between the measured and the simulated resonance frequencies. Therefore, it is not necessary to compute the theoretical values corresponding to the measured frequencies f_{ik} again and again in an iterative way during the minimization of F with respect to the model parameters (X). This is a distinct advantage compared to the method of ref. 5 as has already been outlined by one of the authors⁷. A similarity to the technique of Rizzoli and Lipparini⁷ on the other hand, consists in the fact that the presented method does not rely on a special definition of microstrip characteristic impedance. This can be shown by analytical expansion of the resonance condition (3) as done for the two-port case in ref. 16. Nevertheless, for the purpose of modelling, denormalization is very convenient and helps to visualize results to the microwave engineer. It is performed here employing the power-current formulation of microstrip characteristic impedance^{14,16}. Also, the description of the microstrip gap given here has been obtained from computed scattering parameters by means of this definition.

AN APPLICATION OF THE METHOD

The application of the outlined resonator method to a specific modeling problem is indicated in fig. 3. The discontinuities considered there are the microstrip corner (a) and the chamfered microstrip right-angle bend (b). For both of these, the equivalent circuit (c) is used in accordance with other authors, for example refs. 1,2,4. The degree of chamfer chosen for simplicity in case (b) is 50% which is near the optimum value², and the reference planes RP in fig. 3 are identical with the inner edges of the involved microstrip lines. Fig. 3(d) shows in which way the discontinuities are introduced into the simulation of the associated resonator test measurements. The gap widths and the widths of the lines embedding the structure under test need not be accurately tailored equal in the experiments. The external loading is accounted for by the impedances $Z = 50$ Ohms. A total of nearly 30 test structures with widely varying microstrip widths and three different substrates with nominal dielectric constants of $\epsilon_r = 2.36, 6.0$ and 10.4 have been investigated in the frequency range up to 14 GHz. This is necessary to introduce the functional dependence on width and dielectric constant into the modeling process. At the same time, this has the advantage of averaging out statistical measurement errors.

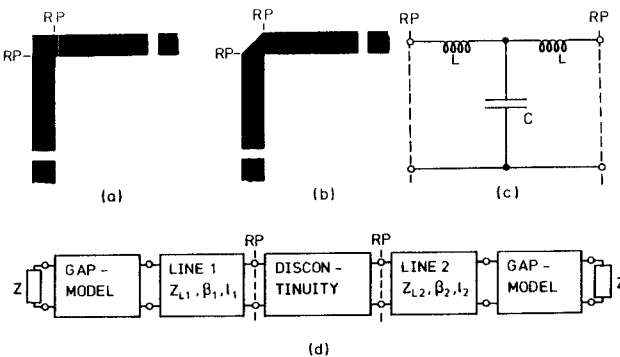


Fig. 3: Test configurations, equivalent circuit and simulation scheme used in the modeling of microstrip corners and chamfered 90°-bends

As a preliminary result of the modeling procedure the elements L and C of the equivalent circuit fig. 3(c) could be obtained for each of the test structures separately by minimizing the error function (4) successively with $M = 1$ for each of these. This is one of the

possibilities to start with if one wants to work out an idea about the behaviour of a model as a function of the physical parameters which are varied in the experiments. In this case, the vector of model parameters (X) constitutes of the elements L and C themselves. In the next step, suitable multidimensional functions are developed and the minimization of F over the whole set of M test configurations is performed. Now, the vector (X) with respect to which the minimum of F has to be found is formed by the degrees of freedom, i.e. weighting factors, coefficients, additive correction terms and so on, implemented into the developed functions. If the latter turn out to be of insufficient accuracy in the optimization they have to be modified so as to achieve better agreement with the measured frequencies. In the specific case of application considered here, the result of such a computer-aided modeling procedure can be given as

$$C/pF = 0.001(h/mm) \cdot ((10.35 \epsilon_r + 2.5) \cdot (w/h)^2 + (2.6 \epsilon_r + 5.64) \cdot (w/h)) \quad (5)$$

$$L/nH = 0.22(h/mm) \cdot (1 - 1.35 \cdot \exp(-0.18(w/h)^{1.39}))$$

for the microstrip corner without chamfering, and as

$$C/pF = 0.001(h/mm) \cdot ((3.93 \epsilon_r + 0.62) \cdot (w/h)^2 + (7.6 \epsilon_r + 3.80) \cdot (w/h)) \quad (6)$$

$$L/nH = 0.44(h/mm) \cdot (1 - 1.062 \cdot \exp(-0.177(w/h)^{0.947}))$$

for the chamfered microstrip right-angle bend. In the frequency range investigated, a noticeable change of the elements L and C with frequency could not be detected. The mathematical models (5) and (6) apply for dielectric constants between about 2 and 13, the range of normalized microstrip widths for which they are valid is $w/h = 0.2 - 6.0$. A comparison with data available from the technical literature^{1,4} reveals close agreement for the capacitance (5). For the associated inductance value L , the deviation is larger, especially for normalized widths of w/h exceeding $w/h = 1$. For both models (5) and (6) developed here, the average relative error by which the measured and the simulated resonance frequencies are different is approximately 0.3%. This is the same order of magnitude as achieved for the basic test configuration of fig. 1 and thus gives confidence in the accuracy of the derived models.

REFERENCES

- 1 K.C.Gupta et al., Artech House, Dedham MA., 1979
- 2 T.C.Edwards, John Wiley, New York, 1981
- 3 T.C.Edwards, IEEE MTT-S Digest, 1982, 338-341
- 4 B.Easter, IEEE Trans., MTT-23, 1975, 655-660
- 5 V.Rizzoli, A.Lipparini, ibid., MTT-29, 1981, 655-660
- 6 L.Gruner, IEEE Trans., IM-30, 1981, 198-201
- 7 R.H.Jansen, mikrowellen mag., Vol.8, 1982, 433-437
- 8 W.J.R.Hoefer et al., IEEE Trans., MTT-23, 1067-1071
- 9 R.H.Jansen, Proc. IEE, MOA-3, 1979, 14-22
- 10 R.H.Jansen, Proc. IEE, Pt.H, 1981, 77-86
- 11 R.H.Jansen et al., Proc. 11th EuMCConf., 1981, 682-687
- 12 M.Kirschning et al., Electronics Letters, Vol.17, 1981, 123-125
- 13 M.Kirschning, R.H.Jansen, Electr. Letters, Vol.18, 1982, 272-273
- 14 R.H.Jansen, M.Kirschning, Electronics and Communications (AEÜ), W.Germany, 1983, 108-112
- 15 N.H.L.Koster, R.H.Jansen, IEEE Trans., MTT-30, 1982, 1273-1279
- 16 R.H.Jansen et al., IEEE MTT-S Digest, 1982, 305-307